Orbital
The electronic journal of chemistry

the electronic journal of chemistry

Full Paper | http://dx.doi.org/10.17807/orbital.v15i1.17592

Investigation of *Neolamarckia cadamba* Phytoconstituents Against SARS-CoV-2 3CL Pro: An In-Silico Approach

Sumit Arora [*a], Kalpana Tirpude [b], Pallavi Rushiya [b], Nidhi Sapkal [c], Subhash Yende [d] Abhay Ittadwar [e], and Sapan Shah [f]

In present study, the inhibitory potential of *Neolamarckia cadamba* phytoconstituents was investigated against SARS-CoV-2 3CL protease (3CL pro) (PDB ID: 6M2N). Molecular docking was analyzed using AutoDock Vina software by setting the grid parameter as X= -33.163, Y= -65.074 and Z= 41.434 with dimensions of the grid box 25 × 25 × 25 Å. Remdesivir was taken as the standard for comparative analysis along with inhibitor 5, 6, 7-trihydroxy-2-phenyl-4H-chromen-4-one. Furthermore, the exploration of 2 D Hydrogen-bond interactions was performed by Biovia Discovery Studio 4.5 program to identify the interactions between an amino acid of target and ligand followed by assessment of physicochemical properties using Lipinski's rule and Swiss ADME database. The decent bonding scores of secondary metabolites owing to hydrogen bonding with catalytic residues suggest the effectiveness of these phytochemicals towards 3CLpro. The results are further consolidated positively by Lipinski's rule and Swiss ADME prediction. Thus reasonably, observations with docking studies suggest possibility of phytochemicals from *Neolamarckia cadamba* to inhibit the 3CLpro and consequently would be explored further as agents for preventing COVID-19.

Graphical abstract

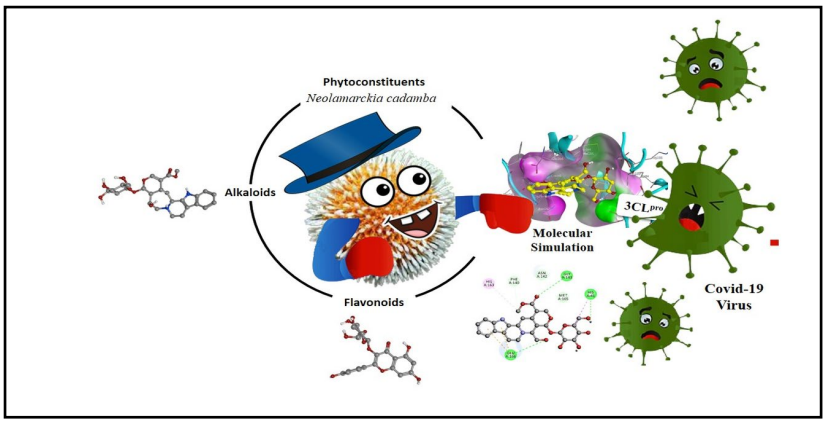

Keywords

3CL Pro
Molecular docking
Neolamarckia cadamba
Phytoconstituents
SARS-CoV-2

Article history

Received 11 Nov 2022
Revised 15 Feb 2023
Accepted 20 Mar 2023
Available online 12 Apr 2023

Handling Editor: Adilson Beatriz

1. Introduction

[a] Department of Pharmacognosy and Phytochemistry, Gurunanak College of Pharmacy, Nari, Nagpur 440026, Maharashtra, India. [b] M. Pharm Research Scholar, Department of Pharmaceutical Chemistry, Gurunanak College of Pharmacy, Nari, Nagpur 440026, Maharashtra, India.[c] Department of Pharmaceutical Chemistry, Gurunanak College of Pharmacy, Nari, Nagpur 440026, Maharashtra, India.[d] Department of Pharmacology, Gurunanak College of Pharmacy, Nari, Nagpur 440026, Maharashtra, India.[e] Gurunanak College of Pharmacy, Nari, Nagpur 440026, Maharashtra, India.[f] Department of Pharmaceutical Chemistry, Priyadarshini J. L. College of Pharmacy, Hingna Road, Nagpur-440016, Maharashtra, India. *Corresponding author, E-mail: **sumitkishanarora@gmail.com**

The unmatched situation created by Coronavirus disease (COVID-19) has unfolded into distressing states of affairs in every walk of life across the globe. It all started with symptoms like common cold, fever, cough, sore throat leading to labored breathing followed by a series of events and eventually death. As of today, 16 February 2023, 75.6 crore people have succumbed to COVID-19 disease with 68.4 lakh death cases. SARS-CoV-2 is a zoonotic transmissible β coronavirus having precedence with MERS-SARS (Middle East Respiratory Syndrome – Severe Acute Respiratory Syndrome) and is closely related to SARS-CoV. Many investigative and exploratory studies have been carried out as part of the efforts to design anti-SARS-CoV-2 drug to target spike protein, non-structural protein, RNA dependent RNA polymerase, and Angiotensin-Converting Enzyme II (ACE-II, the entry receptor for virus). These studies also include the genome part responsible for SARS-CoV-2 replication inside host cell [1]. In confirmation with MERS-SARS, the SARS-CoV-2 has ORF1a and ORF1ab, the Open Reading Frames that translate viral polyproteins pp1a and pp1ab, necessary for viral replication and transcription [2, 3]. The main functional proteins released from pp1a and pp1ab are papain-like proteinase (PLpro) and the 3C-like protease (3CLpro, also called Main protein M^{pro} as it cleaves maximum polypeptide chains). In polyprotein activation and virus maturation, Mpro plays a pivotal role, it is found to be an indispensable target for exploring antiviral drugs against SARS CoV-2 [2, 4]

To defeat this deadly disease, many vaccines have been announced worldwide focusing mainly on the RNA, adenovirus vectors, spike-like protein, nucleic acids, inactivated viruses, etc.[5]. From April 2021, National Regulatory Authority (NRA) has approved 12 vaccines targeting diverse factors, Pfizer-BioNTech and Moderna for RNA mutant, Sputnik V, J & J, Oxford- AstraZeneca and Convidecia for adenovirus vector, Covaxin, CoronaVac, Sinopharm (BBIBP), Sinopharm (WIBP), CoviVac and QazVac for inactivated virus and two protein subunit vaccines viz. EpiVacCorona and RBD-Dimer for the public use [6, 7]. Many existing drugs like Lopinavir, Oseltamivir, Ritonavir, and Favipiravir have been tested computationally against SARS-CoV-2 protease enzymes, as repurposing and computational studies save cost, time, and risks [8, 9]. Food and Drug Administration (FDA) has also permitted a range of drugs like Remdesivir, Oseltamivir, Doxycycline, Hydroxychloroquine, Ivermectin, Favipiravir, and many more for curing Covid 19[10]. However, No precise medications are available for COVID-19 treatment, hence there is a need to develop safe and effective drugs on a priority basis [11]. As plant-based drugs or herbal extracts have less toxicity and are safe to use, as compared to synthetic drugs, therefore, many bioactive compounds derived from plants have attracted researchers to study their antiviral activities against SARS-CoV-2 [12–14].

Considering the grim consequences of increased number of active cases at the current time, computer-aided drug design (CADD) is preferred approach for developing new drug treatments. The CADD approaches minimize the time and expenditure required for drug research. It is mainly based on molecular docking to identify lead molecules against the target proteins from the available chemical compounds [15, 16]. The molecular docking is a simulation technique used to study the protein-ligand interactions. In molecular docking simulations, many ligand poses are formed inside the binding pocket of protein molecule, out of which best poses are evaluated with the help of scoring functions and binding interactions [17]. This docking score is obtained based on thermodynamic energy terms in the receptor-ligand binding [18–20]. AutoDock (version 4.2.6) and Autodock Vina are popularly used tools for molecular docking simulation studies. Thermodynamically meaningful energy terms, i.e., intermolecular energy term and torsion energy are utilized in generating binding energy scores in AutoDock and Autodock Vina. Intermolecular binding energy considers H-bonds, Van der Waal's interaction, desolvation energy, and electrostatic potential in the protein-ligand interaction. The torsion energy term integrates the free energy released in ligands due to the rotational bonds [21, 22].

Neolamarckia cadamba (*N. cadamba*) (family: Rubiaceae) commonly recognized as "Kadamba" in India, is a perennial tropical tree found in different parts of the world. It is popular for its numerous medicinal properties viz., Antivenom [23], Antioxidant [24], Antimicrobial [25], Antifungal [26], Antitumor [27], Antihepatotoxic [28], Diuretic and laxative activity [29], Hypolipidemic [30]. The reported phytoconstituents of this plant are cadambagenic acid, cadamine, quinovic acid, β-sitosterol, cadambine, dihydrotectochrysin, dihydrowogonin, pinocembrin, chrysin, naringenin, kaempferol, aromadendrin, quercetin, taxifolin, Narigenin, apigenin, β-sitosterol, sakuranetin, prunetin, 7-O-(β-D-glucopyranosyl)-5-O-methylnaringenin, genistein, prunetin, n-pentacosane, triacontane, noctacosanol, β-sitosterol, sakuranetin, puddumetin, flavanone, sakuranetin, etc. [24, 31, 32].

Several studies report the therapeutic potential of this plant in the above mentioned diseases and no studies are reported regarding its use in corona virus infections The inspiration for exploring the use of this plant was derived from the fact that Cadamba flowers have spiky hairy structure resembling the structure of Coronavirus. In nature there are several examples where the similarity of looks can be attributed to their role. Hence, due to this similarity it was thought to identify the phytochemicals from *N. cadamba* that might have activity against the Coronavirus using the molecular docking method.

2. Material and Methods

2.1 Platform for molecular docking

The computational docking of all the phytoconstituents selected as ligands with target 3CL pro was done through AutoDock Vina software [22, 33].

2.2 Protein preparation

In-silico investigation of selected phytoconstituents was performed on the 2.20 Å crystal structure of 3CL pro with inhibitor 5,6,7-trihydroxy-2-phenyl-4H-chromen-4-one (PDB ID: 6M2N, having resolution 2.20 Å, R-Value Free <0.26, R-Value Work<0.23) which was retrieved from protein data bank (https://www.rcsb.org). Chains A, B, C, and D were used for macromolecule preparation, non-standard residues, co-crystallized water molecules, and unwanted chains identified as undesirable residues and were removed. UCSF chimera tool, Dock-prep was utilized for energy minimization and geometry optimization. Further, Gasteiger, polar hydrogen, and partial charges were allocated to atoms to produce a protonation state at physiological pH respectively [34].

2.3 Ligand preparations

The two-dimensional (2D) structure files of all

phytoconstituents selected as ligand molecules were acquired from National Centre for Biotechnology Information (NCBI) maintained PubChem database (https://pubchem.ncbi.nlm.nih.gov) via UCSF chimera software (v.1.14). The 2D structures were converted into three-dimensional (3D) structures through Marvin program converter module and the files were saved in MOL format. Further, Energy minimization of all ligands was achieved using Amber ff12SB force field UCSF Chimera v.1.14 software [35].

2.4 Molecular Docking

To study the interaction between the phytoconstituents and 3CLpro (6M2N), docking studies were performed and the binding energy of the protein-ligand complex was determined [36, 37]. AutoDock Vina [38] tool integrated with UCSF Chimera software v1.14 [39] was utilized applying the default values for the parameters, and a grid box (25 × 25 × 25) A˚ centered at (-33.163 × -65.074 × 41.434) A˚ with 0.375 Å of grid spacing. The binding affinity was explored using the View Dock tool. The docking results were seen using the 'View Dock' tab. Visualization of obtained docked conformation was studied using Discovery Studio 2020 Client [40] and PyMol software [41].

2.5 ADME and Toxicity prediction

Lipinski's rule of five was utilized for the calculation of drug-likeness properties of selected phytoconstituents. Swiss ADME **(http://www.swissadme.ch)** an online server database was utilized to assess the pharmacokinetic profile (ADME) and Toxicity predictions of ligands. To analyze toxicological properties of ligands, SMILES notations or SDF files were uploaded. Subsequently required models for generating information about structure-related effects were selected [33, 42].

3. Results and Discussion

Exploring the potential of known chemical compounds including phytoconstituents in SARS CoV-2 [43] has become a worldwide tactic [44, 45]. Use of molecular docking techniques makes this exploration easier, faster and reliable. Molecular docking study provides insight on a molecular mechanism involving binding of a ligand with target protein and therefore this could give a notion to modify, optimize, validate the molecules and implement for drug design [46]. SARS Cov-2 3CLpro cleaves the viral polyprotein at 11 different sites and generates non-structural proteins responsible for the formation of new RNA virus [4]. Amongst the coronavirus targets, this protein is considered a selective target [47]. The earlier literatures have established the potential of baicalein as anti-SARS CoV-2 drug. PDB Id 6M2N was selected for docking studies as its structure contained baicalein as the native ligand. Baicalein is a small flavonoid molecule and knowledge of the binding mode of this flavonoid structure with 6M2N can be useful in studying the anti-SARSCoV-2 potential of the phytoconstituents of *N. cadamba* [46, 48].

The molecular docking study was initiated by redocking the native ligand for identifying the docking pose and validating the computer model. The RMSD value of redocked poses was 2.446 Å for 6M2N. A great deal of similarity was found between the original and the redocked pose. Consequently, these docking parameters were further utilized for calculating the binding energies of Standard compound and phytoconstituents. The native ligand, baicalein shows binding energy-7.2 kcal/mol contributed by hydrogen binding with MET-49 and other interaction with catalytic residue CYS-145 [49] along with MET-165, CYS-44 and ASN-142 demonstrating the effectiveness of ligand binding with target protein [50] (Figure 1). As reference drug, Remdesivir (-7.1 kcal/mol) lacks the hydrogen bonding with catalytic dyad but demonstrates a useful interaction with PHE-140, LEU-141, SER-144, HIS-163, HIS-164, ASN-142, and hydrophobic interaction as that of the native ligand with missing one or more residue with each other (Figure 1). This result was in coherence with the previously reported literature suggesting PHE-140 and LEU-141 as important interaction residues of 3CLpro [45, 51].

The docking scores of phytoconstituents as ligands from *N. Cadamba* which showed good binding affinity and prominent interaction have been provided in Table 1 (**Supporting Information**). Amongst the phytoconstituents, Rutin, a natural flavone derivative showed the highest binding affinity -8.7 kcal/mol contributed by hydrogen bonding with GLU-166, LEU-167, TYR-54, ASN-142, THR-26, CYS-44, MET-49 and non-bonding interaction involving hydrophobic characters with GLN-189, HIS-41 (Figure 2 and 3). A similar study proposed by Bala Sivani et al reported the involvement of this interacting residue with Rutin from *Moringa oleifera* for inhibition of SARS-CoV-2 main protease [52]. Glycosyloxy flavone, Afzelin demonstrates – 8.5 kcal/mol binding energy when interacting with 3CLpro at vital interacting residues such as LEU-141, CYS-44, TYR-54, HIS-41, HIS-163, ASN-142, MET-49 and hydrophobic interaction with catalytic residue CYS-145 (Figure 2 and 3). While Quercetin, Kaempferol, and Kaempferol-3O-glucoside showed hydrogen bonding with catalytic site HIS-41, CYS 145, and hydrophobic interaction with a prominent residue having binding score – 7.9 kcal/mol, – 7.7 kcal/mol and – 8.1 kcal/mol respectively (Figure 2 and 3). The earlier result also mentioned the inhibitory potential (IC50: 23.8 μM) of quercetin against SARS-CoV 3CLpro [53]. Likewise, Naringenin, flavanones molecule showed hydrophobic interaction with catalytic dyad CYS-145 and HIS-41 along with HIS-163, MET-165 with binding score -7.5 kcal/mol (Figure 2 and 3). The above observations confirmed that most of the phytoconstituents with favourable binding affinities are regarded as flavonoids and have shown the prospective to establish strong interaction with the target protein and so was the result for other flavonoids like Apigenin, Leucocyanidine, Genkwanin, Catechin, Pinocembrin, Aromadendrine, Taxifolin, Sakuranetin, etc. Similar results were reported for Rutin, Isorhamnetin-3-O-rutinoside, Quercetin-3-gentiobioside, Ellagic acid, and Apigenin-7-O-rutinoside from *Moringa oleifera* flavonoid phytoconstituents to have inhibitory action against the target Main protease SARS-CoV-2 through molecular docking, ADMET and dynamics studies [52, 54]. Furthermore, the presence of chromene nucleus and flavonoid moiety was also found as potential inhibitors of SARS-CoV-2 3CLpro [46].

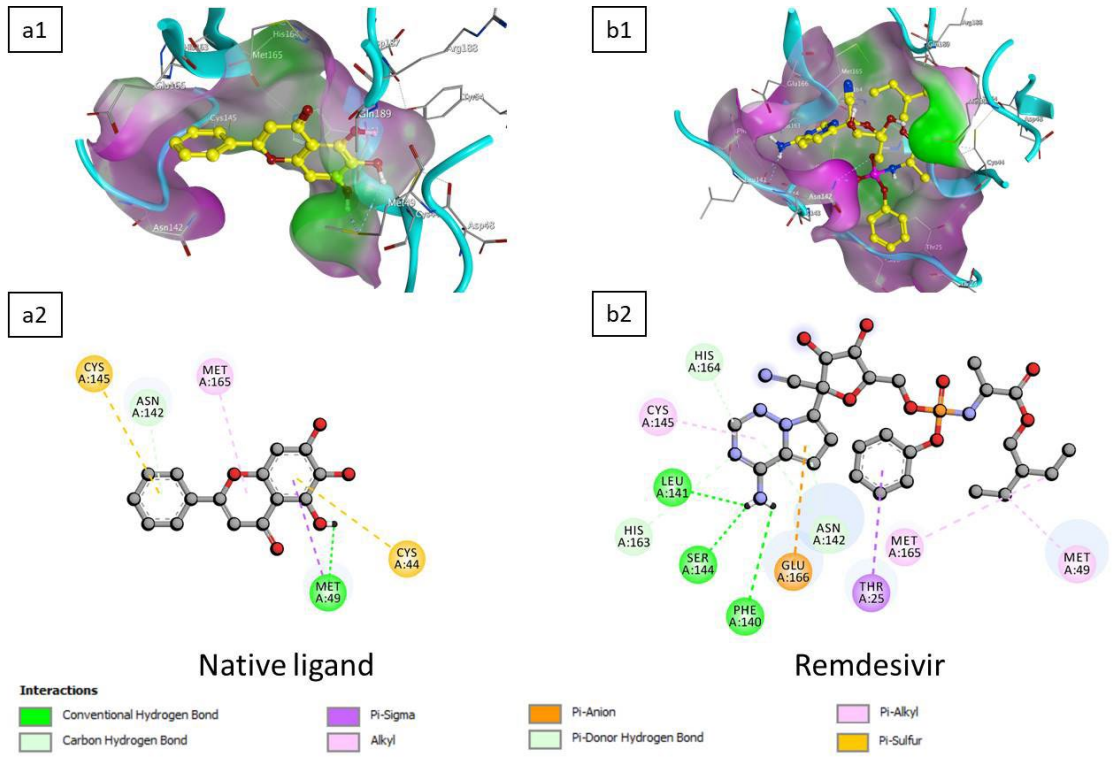

Fig. 1. Docked poses (3D and 2D) of native ligand (3WL) and standard drug Remdesivir in the binding pocket of 3CL^{pro} crystal (PDB ID: 6M2N). 3D pose (a1 and b1): ligand is represented in ball and sticks model, interacting amino acid residues in lines, H-Bonds are represented by cyan dashed lines and the H-pi-Bonds as lime dashed lines. The poses are overlaid with molecular surfaces according to lipophilicity (green-Lipophilic, white-neutral, and magenta-hydrophilic regions). 2D pose (a2 and b2): Ligand is represented in the ball and stick model, interacting amino acids in circles, Conventional hydrogen bonds are represented by green dashed lines; Carbon and π-donor hydrogen bonds as light green, Attractive electrostatic interactions as orange dashed lines; alkyl and π-alkyl interactions as pink and purple dashed lines.

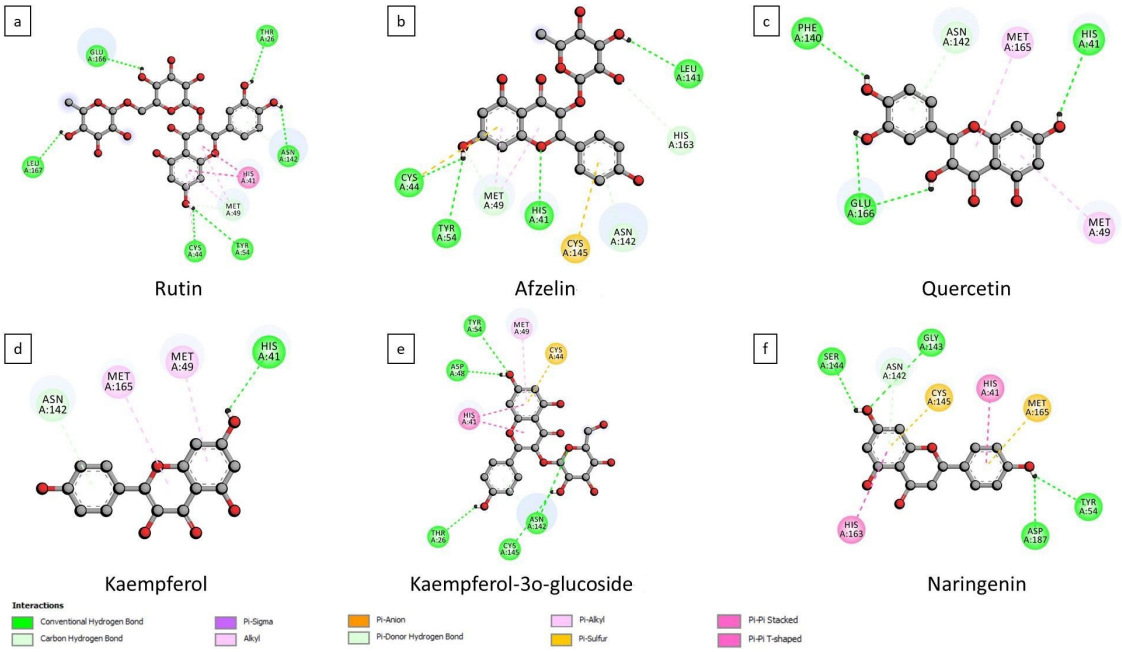

Fig. 2. 2D binding interactions of a) Rutin b) Afzelin c) Quercetin d) Kaempferol e) Kaempferol-3o-glucoside f) Naringenin against 3CL^{pro} of SARS-CoV-2 (PDB ID: 6M2N). Ligand is represented in the ball and stick model, interacting amino acids in circles, Conventional hydrogen bonds are represented by green dashed lines; Carbon and π-donor hydrogen bonds as light green, Attractive electrostatic interactions as orange dashed lines; alkyl and π-alkyl interactions as pink and purple dashed lines.

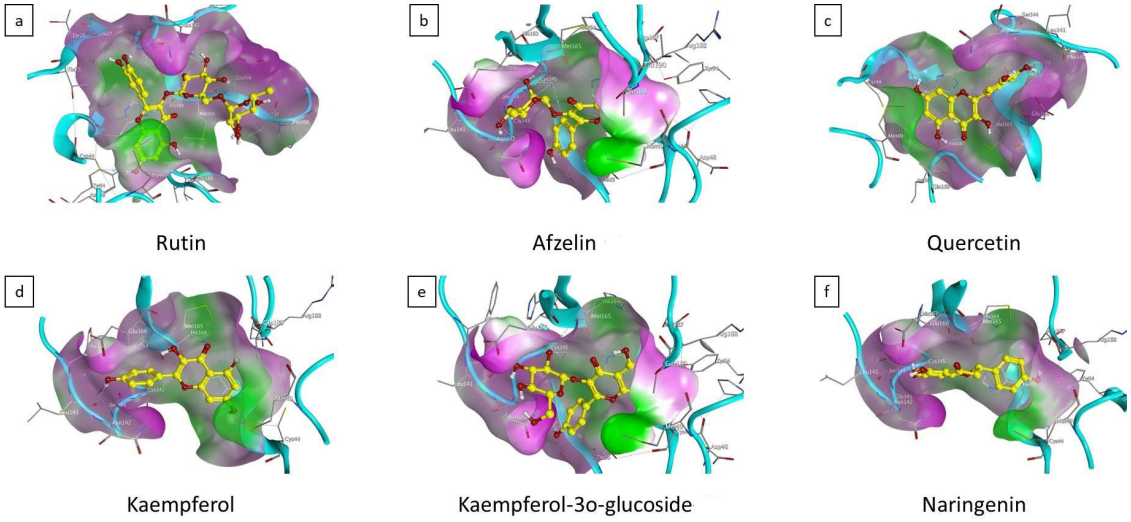

Fig. 3. 3D docked poses and binding interactions of a) Rutin b) Afzelin c) Quercetin d) Kaempferol e) Kaempferol-3o-glucoside f) Naringenin against 3CL^{pro} of SARS-CoV-2 (PDB ID: 6M2N). Ligand is represented in the ball and sticks model, interacting amino acid residues in lines, H-Bonds are represented by cyan dashed lines, and the H-pi-Bonds as lime dashed lines. The poses are overlaid with molecular surfaces according to lipophilicity (green-Lipophilic, white-neutral, and magenta-hydrophilic regions).

Consequently, alkaloids phytoconstituents Cadambine and its derivatives such as Cadambine Acid, Isodihydrocadambine, Dihydrocadambine, Beta Dihydro Cadambine, Aminocadambine A, Aminocadambine B demonstrated good binding affinity as evident from their docking score -7.6, -7.7, -8.3, -8.3, -8.3, -8.0 and -8.4 kcal/mol respectively. Amongst them, Isodihydrocadambine, Dihydrocadambine, and Beta Dihydro Cadambine showed hydrogen bonding with HIS-41, MET-49, GLN-189, and GLY-143 along with hydrophobic interaction with vital interacting residue HIS-163 and PHE-140 revealed its strength as 3CLpro inhibitors (Figure 4 and 5). The plethora of results reported for alkaloids as Potential Phytochemicals against SARS-CoV-2 via interfering viral replication [55–57]. Moreover, Chlorogenic acid, phenolic secondary metabolites have shown hydrogen bonding with MET-49, THR-25, CYS-145, and GLY-143 and hydrophobic interaction with THR-26 and HIS-41 having a docking score of -7.3 kcal/mol (Figure 4 and 5). Earlier findings also reported the efficiency of Chlorogenic acid as a potential inhibitor of SARS-CoV-2 infection [58]. Likewise 2'-hydroxy-2,4,4',5-tetramethoxy Chalcone demonstrated its effectiveness with a binding score of -7.1 kcal/mol contributed by hydrogen bonding with catalytic residue HIS-41 and non-bonding interaction involving hydrophobic characters with MET-49, MET-165, GLU-166, LEU-167, THR-25, and SER-49 (Figure 4 and 5). Recent findings by Nizami Duran *et al*. also proved the usefulness of Chalcone and its derivatives against SARS-CoV-2 [59]. Similarly, anthraquinone derivatives like Emodine, Physcion, and Chrysophanol have been found to interact with 3CLpro at vital interacting residues such as HIS-41, CYS-145, MET-49, GLN-189, CYS-44, and ASP-187 exhibited by binding energies of -7.8, -7.5 and -7.5 kcal/mol respectively (Figure 6). Previous findings also mentioned the anthraquinone derivatives as immune booster molecules and having a therapeutic efficacy against COVID-19 infection [60].

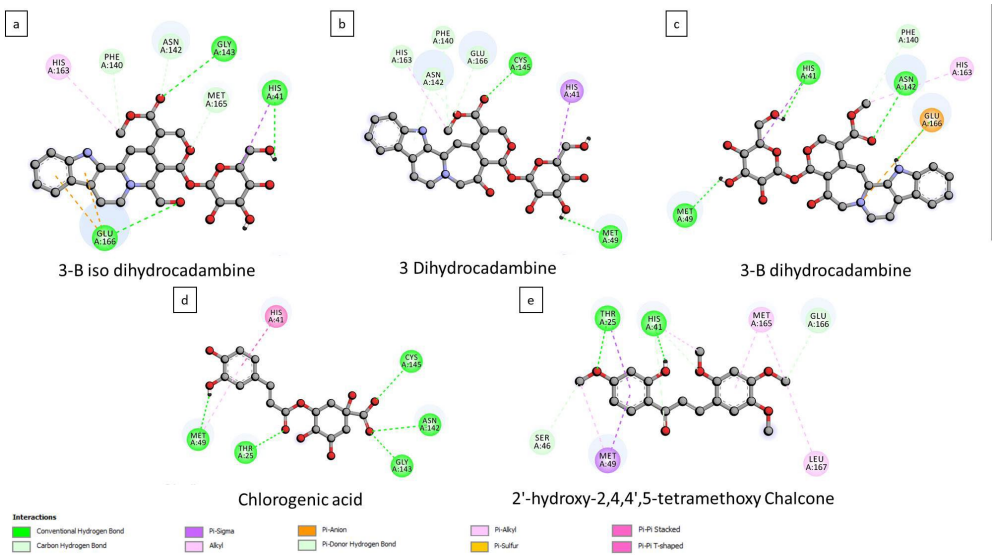

Fig. 4. 2D binding interactions of a) 3-B Isodihydrocadambine b) 3-dihydroadambine c) 3-B dihydrocadambine d) Chlorogenic acid e) 2'-hydroxy-2,4,4',5-tetramethoxy Chalcone against 3CL^{pro} of SARS-CoV-2 (PDB ID: 6M2N). Ligand is represented in the ball and stick model, interacting amino acids in circles, Conventional hydrogen bonds are represented by green dashed lines; Carbon and π-donor hydrogen bonds as light green, Attractive electrostatic interactions as orange dashed lines; alkyl and π-alkyl interactions as pink and purple dashed lines.

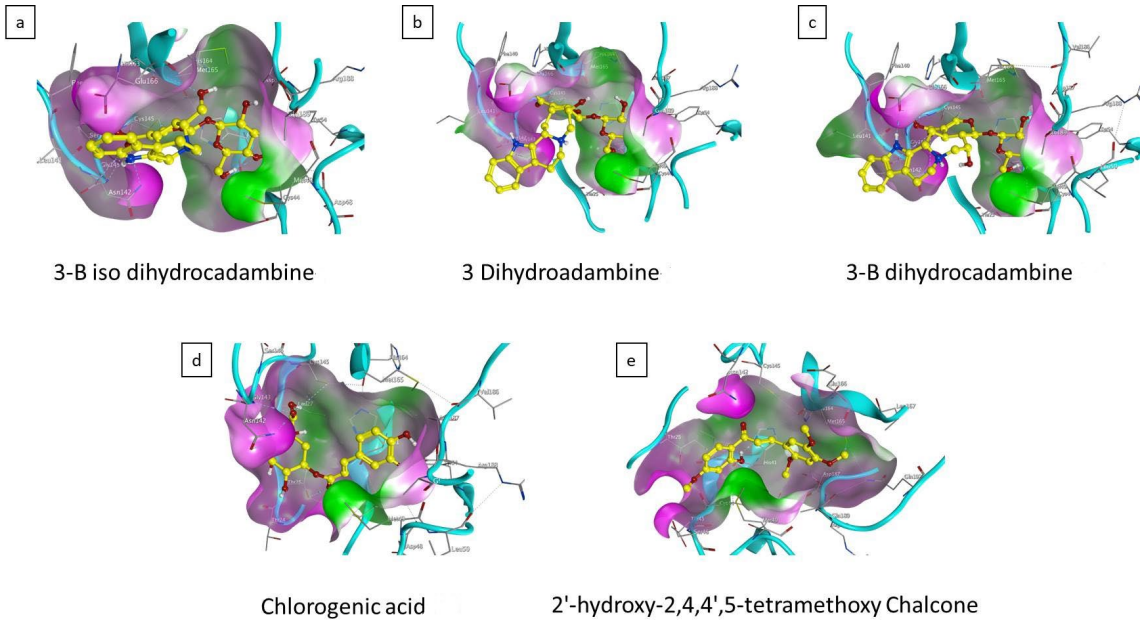

Fig. 5. 3D docked poses and binding interactions of a) 3-B Isodihydrocadambine b) 3-dihydroadambine c) 3-B dihydrocadambine d) Chlorogenic acid e) 2'-hydroxy-2,4,4',5-tetramethoxy Chalcone against 3CL^{pro} of SARS-CoV-2 (PDB ID: 6M2N). Ligand is represented in the ball and sticks model, interacting amino acid residues in lines, H-Bonds are represented by cyan dashed lines, and the H-pi-Bonds as lime dashed lines. The poses are overlaid with molecular surfaces according to lipophilicity (green-Lipophilic, white-neutral, and magenta-hydrophilic regions).

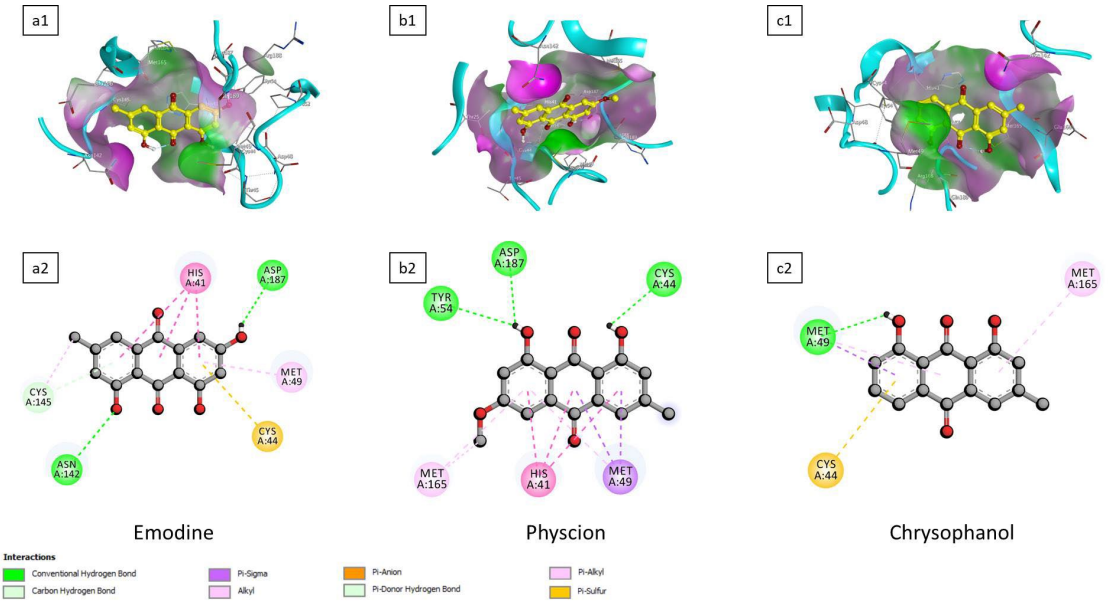

Fig. 6. Docked poses (3D and 2D) of Emodine (a1 and a2), Physcion (b1 and b2), and Chrysophanol (c1 and c2) in the binding pocket of 3CL^{pro} crystal (PDB ID: 6M2N). 3D pose (a1, b1, and c1): ligand is represented in ball and sticks model, interacting amino acid residues in lines, H-Bonds are represented by cyan dashed lines and the H-pi-Bonds as lime dashed lines. The poses are overlaid with molecular surfaces according to lipophilicity (green-Lipophilic, white-neutral, and magenta-hydrophilic regions). 2D pose (a2, b2, and c2): Ligand is represented in the ball and stick model, interacting amino acids in circles, Conventional hydrogen bonds are represented by green dashed lines; Carbon and π-donor hydrogen bonds as light green, Attractive electrostatic interactions as orange dashed lines; alkyl and π-alkyl interactions as pink and purple dashed lines.

The above observation perpetuates that the majority of secondary metabolites from *N. Cadamba* possibly will be used as an alternative therapy for the management of SARS-CoV-2 infection. In addition, we have investigated the Drug-likeness and ADME properties of the above phytoconstituents using the Lipinski rule and SwissADME as these parameters play a critical role in drug development and their values were depicted in Table 2 (**Supporting Information**). Lipinski's rules describe any drug having a molecular weight (MW) of < 500 Da, a polar surface area (PSA) of < 150 Å, an octanol-water partition coefficient (log P) of < 5, number of hydrogen bond acceptors (HBAs) < 10, number of hydrogen bond donors (HBDs) <5 and number of rotatable bonds (RBs) < 10 is recognized as a good molecule in terms of oral activity. Compounds violating more than two rules out of five were not considered for drug-likeness

irrespective of having a strong binding affinity with the target protein [61]. Amongst them, 60 % of Phytochemicals suggested above as potential inhibitors against 3CLpro, follows Lipinski's rule of five, although some of them may infringe with 1 or 2 violation. Furthermore, along with drug-likeness, ADME properties provide insight into the synthesis of a drug molecule and its development for further research and are reflected as significant criteria to understand the physicochemical and pharmacokinetic properties [62]. According to the Silicos-IT score, 54.54 % of the screened phytochemicals were classified as soluble, 43.63% moderately soluble and 3.63 % classified as poorly soluble suggesting the good solubility of phytomolecules. Earlier findings suggest that compounds should have a bioavailability score of 0.55 or 0.56 for good pharmacokinetic properties [63]. Likewise in our study, 83.63 % of phytochemicals compounds have (a 0.55 score) indicating better bioavailability, 7.27 % of phytochemicals (4-Caffeyolsweroside, Cadambine, Feruloylquinic Acid, Cadambine Acid) has less score (0.11 score) and 5.45 % of ligands (3- Oleic Acid, Ursolic Acid, Palmitic Acid) shows 0.85 respectively. Furthermore, amongst phytochemicals, 54.54 % showed high GI absorption. Altogether, from the above observation, we put forward that these phytochemicals have the possible capacity to function effectively as drugs

4. Conclusions

In existing conditions of COVID-19 across the sphere and the unavailability of specific treatment for the SARS-CoV-2 virus has upraised concern among the people worldwide that demand alternative options to combat this disease. Traditional plants have been reflected as a rich source of phytochemicals for various diseases. In our present investigation, we docked the numerous phytochemicals from *N. Cadamba* against 3CLpro and our result provides insights into the effectiveness of phytochemicals. The results also extend that majority of secondary metabolites such as flavonoids, chalcone, alkaloids, anthraquinone, etc. from *N. Cadamba* demonstrated the good binding scores contributed by hydrogen bonding with catalytic residues. In addition, these phytochemicals could effectively function as drugs revealed from the results of Lipinski's rule of five and SwissADME prediction. Thus, the outcomes of our study suggest that phytochemicals from *N. cadamba* have the potential to inhibit the 3CLpro and therefore should be explored further as agents for preventing COVID-19.

Supporting Information

Table 1: Molecular Docking of Cadamba phytochemicals with 6M2N Sars Cov-2 Protein. Table 2: Physiochemical properties of Phytochemicals

Acknowledgments

The authors are thankful to the management of the Sikh Education Society for extending facilities and providing necessary support.

Author Contributions

Sumit Arora, Kalpana Tirpude, and Pallavi Rushiya contributed to molecular docking, analysis of the data, and draft of the paper. The concept study was designed and supervised by Sapan Shah and Subhash Yende. Nidhi Sapkal and Abhay Ittadwar contributed to the critical reading and editing of the manuscript. All the authors have read and agreed to the manuscript for submission.

References and Notes

[1] Hasan, A.; Paray, B. A.; Hussain, A.; Qadir, F. A.; Attar, F.; Aziz, F. M. *J. Biomol. Struct. Dyn.* **2020**, *1*. [Crossref]

[2] Grum-Tokars, V.; Ratia, K.; Begaye, A.; Baker, S. C.; Mesecar, A. D. *Virus Res.* **2008**, *133*, 63. [Crossref]

[3] Boopathi, S.; Poma, A. B.; Kolandaivel, P. *J. Biomol. Struct. Dyn.* **2020**, 1. [Crossref]

[4] Anand, K.; Ziebuhr, J.; Wadhwani, P.; Mesters, J. R.; Hilgenfeld, R. *Science* **2003**, *300*, 1763. [Crossref]

[5] Meo, S. A.; Bukhari, I. A.; Akram, J.; Meo, A. S.; Klonoff, D. C. *Eur. Rev. Med. Pharmacol. Sci.* **2021**, *25*, 1663.

[6] Lakhera, S.; Devlal, K.; Ghosh, A.; Rana, M. *Results Chem.* **2021**, *3*, 100199. [Crossref]

[7] McIntyre, P.; Joo, Y. J.; Chiu, C.; Flanagan, K.; Macartney, K. *Aust. Prescr.* **2021**, *44*, 19. [Crossref]

[8] Xue, H.; Li, J.; Xie, H.; Wang, Y. *Int. J. Biol. Sci.* **2018**, *14*, 1232. [Crossref]

[9] Muralidharan, N.; Sakthivel, R.; Velmurugan, D.; Gromiha, M. M. *J. Biomol. Struct. Dyn*. **2020**, *39*, 2673. [Crossref]

[10] Zuckerman, D. M. *Am. J. Public Health* **2021**, *111*, 1065. [Crossref]

[11] Enayatkhani, M.; Hasaniazad, M.; Faezi, S.; Gouklani, H.; Davoodian, P.; Ahmadi, N. *J. Biomol. Struct. Dyn.* **2020**, *39*, 2857. [Crossref]

[12] Sawikowska, A. *Biometrical Lett.* **2020**. [Crossref]

[13] Jo, S.; Kim, S.; Shin, D. H.; Kim, M. S. *J. Enzyme Inhib. Med. Chem.* **2020**, *35*, 145. [Crossref]

[14] Liu, A. L.; Du, G. H. Antiviral Properties of Phytochemicals BT - Dietary Phytochemicals and Microbes. In: Patra AK (ed). Dordrecht: Springer Netherlands, 2012, p. 93-126.

[15] Meng, X. Y.; Zhang, H. X.; Mezei, M. *Curr. Comput. Aided. Drug. Des*. **2011**, *7*, 146. [Crossref]

[16] Sethi, A.; Joshi, S.K. Molecular Docking in Modern Drug Discovery: Principles and Recent Applications. In: Drug Discovery and Development, IntechOpen, 2019.

[17] Ferrara, P.; Gohlke, H.; Price, D. J.; Klebe, G.; Brooks, C. L. *J. Med. Chem.* **2004**, *47*, 3032. [Crossref]

[18] Smith, R.D.; Dunbar, J.B.; Ung, P.M.U.; Esposito, E.X.; Yang, C.Y.; Wang, S. *J. Chem. Inf. Model* **2011**, *51*, 2115. [Crossref]

[19] Gaieb, Z.; Liu, S.; Gathiaka, S.; Chiu, M.; Yang, H.; Shao, C. *J. Comput. Aided Mol. Des.* **2018**, *32*, 1. [Crossref]

[20] Pagadala, N. S.; Syed, K.; Tuszynski, *J. Biophys. Rev.* **2017**, *9*, 91. [Crossref]

[21] Huey, R.; Morris, G. M.; Olson, A. J.; Goodsell, D. S. *J. Comput. Chem.* **2007**, *28*, 1145. [Crossref]

[22] Morris, G. M.; Huey, R.; Lindstrom, W.; Sanner, M. F.; Belew, R. K.; Goodsell, D. S. *J. Comput. Chem.* **2009**, *30*, 2785. [Crossef]

[23] Lakhmale, S.; Acharya, R.; Yewatkar, N. *Ayurpharm Int. J. Ayur. Alli. Sci.* **2012**, *1*, 21.

[24] Ganjewala, D.; Tomar, N.; Gupta, A. K. *J. Biol. Act. Prod. from Nat.* **2013**, *3*, 232. [Crossref]

[25] Dogra, S. C. *Indian J. Hist. Sci.* **1987**, *22*, 164.

[26] Divyakant, A.; Dirji, V.C.; Bariya, A. H.; Patel, K. R.; Sonpal, R. N. *Int. Res. J. Pharm.* **2011**, *2*, 192.

[27] Dolai, N.; Karmakar, I.; Suresh Kumar, R. B.; Kar, B.; Bala, A.; Haldar, P. K. *J Ethnopharmacol* **2012**, *142*, 865. [Crossref]

[28] Kapil, A.; Koul, I. B.; Suri, O. P. *Phyther. Res.* **1995**, *9*, 189. [Crossref]

[29] Mondal, S.; Dash, G.; Acharyya, A.; Acharyya, S.; Sharma H. *Drug Invent. Today* **2009**, *1*, 78.

[30] Kumar, V.; Mahdi, F.; Chander, R.; Singh, R.; Mahdi, A. A.; Khanna, A. K.; *Indian J. Biochem. Biophys.* **2010,** *47*, 104.

[31] Dwevedi, A.; Sharma, K.; Sharma,Y. K.; *Pharmacogn. Rev.* **2015**, *9*, 107. [Crossref]

[32] Dubey, A.; Nayak, S.; Goupale, D. C. *Pharmacogn. J.* **2011**, *2*, 71. [Crossref]

[33] Arora, S.; Lohiya ,G.; Moharir, K.; Shah ,S.; Yende, S. *Digit. Chinese Med.* **2020**, *3*, 239. [Crossref]

[34] Pettersen, E. F.; Goddard, T. D.; Huang, C.; Couch, G. S.; Greenblatt, D. M.; Meng, E.C. *J. Comput. Chem.* **2004**, *25*, 1605. [Crossref]

[35] Yousuf, Z.; Iman, K.; Iftikhar, N.; Mirza, M. U. *Breast Cancer* **2017**, *9*, 447. [Crossref]

[36] Verdonk, M. L.; Cole, J. C.; Hartshorn, M. J.; Murray, C.W.; Taylor, R.D. *Proteins Struct. Funct. Bioinforma.* **2003**, *52*, 609. [Crossref]

[37] Leach, A. R.; Shoichet, B. K.; Peishoff, C. E. *J. Med. Chem.* **2006,** *49*, 5851. [Crossref]

[38] Trott, O.; Olson, A. J. *J. Comput. Chem.* **2010**, *31*, 455. [Crossref]

[39] Edgar, R. C.; Haas, B. J.; Clemente, J. C.; Quince, C.; Knight, R. *Bioinformatics* **2011**, *27*, 2194. [Crossref]

[40] Biovia, D. S. Discovery Studio Modeling Environment, Release San Diego: Dassault Systèmes, 2017.

[41] DeLano, L. W. Pymol: An open-source molecular graphics tool. {CCP4} *Newsl Protein Crystallogr,* 2002.

[42] Shah, S.; Chaple ,D.; Arora, S.; Yende, S.; Moharir, K.; Lohiya, G. *Netw. Model Anal. Heal. Informatics. Bioinforma.* **2021**, *10*, 8. [Crossref]

[43] Khan, R. J.; Jha, R. K.; Amera, G. M.; Jain, M.; Singh, E.; Pathak, A.; Singh, R. P.; Muthukumaran, J.; Singh, A. K. *J. Biomol. Struct. Dyn*. **2021**, *39*, 2679. [Crossref]

[44] Pushpakom, S.; Iorio, F.; Eyers, P. A.; Escott, K. J.; Hopper, S.; Wells, A. *Nat. Rev. Drug Discov.* **2019**, *18*, 41. [Crossref]

[45] Said, M. A.; Albohy, A.; Abdelrahman, M. *Eur. J. Pharm. Sci. Off. J. Eur. Fed. Pharm. Sci.* **2021**, *160*, 105744. [Crossref]

[46] Said, M. A.; Albohy, A.; Abdelrahman, M. A.; Ibrahim, H. S.; *Results Chem.* **2021**, *3*, 100195. [Crossref]

[47] Ullrich, S.; Nitsche, C. *Bioorg. Med. Chem. Lett.* **2020**, *30*, 127377. [Crossref]

[48] Su, H. X.; Yao, S.; Hao, W. F.; Li, M. J.; Liu, J.; Shang, W. J. *Acta. Pharmacol. Sin.* **2020**, *41*, 1167. [Crossref]

[49] Ferreira, J. C.; Fadl, S.; Villanueva, A. J.; Rabeh, W. M. *Front. Chem.* **2021**, *9*, 692168. [Crossref]

[50] Jain, R.; Mujwar, S. *Struct. Chem.* **2020**, *31*, 24871. [Crossref]

[51] Chatterjee, S.; Maity, A.; Chowdhury, S.; Islam, M. A.; Muttinini, R. K.; Sen, D. *J. Biomol. Struct. Dyn.* **2021,** *39*, 5290. [Crossref]

[52] Sivani, B.; Venkatesh, P.; Murthy, T.; Kumar, S. *Curr. Res. Green Sustain. Chem.* **2021,** *4*, 100202. [Crossref]

[53] Pillaiyar, T.; Manickam, M.; Namasivayam, V.; Hayashi, Y.; Jung, S. H. *J. Med. Chem.* **2016**, *59*, 6595. [Crossref]

[54] Saraswat, J.; Singh, P.; Patel, R. *J. Mol. Liq.* **2021**, *326*, 115298. [Crossref]

[55] Wink, M. *Diversity* **2020**, *12*. 175. [Crossref]

[56] Majnooni, M. B.; Fakhri, S.; Bahrami, G.; Naseri, M.; Farzaei, M. H.; Echeverría J. *Evid.-based Complement. Altern. Med.* **2021**, 6632623. [Crossref]

[57] Pandeya, K. B.; Ganeshpurkar, A.; Mishra, M. K. *Med. Hypotheses* **2020**, *144*, 109905. [Crossref]

[58] Wang, W. X.; Zhang, Y. R.; Luo, S. Y.; Zhang, Y. S.; Zhang, Y.; Tang, C. *Nat. Prod. Res.* **2022**, *36,* 2580. [Crossref]

[59] Duran, N.; Polat, M. F.; Aktas, D. A.; Alagoz, M. A.; Ay, E.; Cimen, F. *Int. J. Clin. Pract.* **2021**, *75*, 14846. [Crossref]

[60] Khanal, P.; Patil, B. M.; Chand, J.; Naaz, Y. *Nat. Products Bioprospect.* **2020,** *10*, 325. [Crossref]

[61] Lipinski, C. A. *Drug Discov. Today Technol.* **2004**, *1*, 337. [Crossref]

[62] Nallusamy, S.; Mannu, J.; Ravikumar, C.; Angamuthu, K.; Nathan, B.; Nachimuthu, K.; Ramasamy, G.; Muthurajan, R.; Subbarayalu, M.; Neelakandan, K. *Front. Pharmaco.* **2021**, *12*, 667704. [Crossref]

[63] Bojarska, J.; Remko, M.; Breza, M.; Madura, I. D.; Kaczmarek, K.; Zabrocki, J. *J. Molecules* **2020**, *25*. [Crossref]

How to cite this article

Arora, S.; Tirpude, K.; Rushiya, P.; Sepkal, N.; Yende, S.; Ittadwar, A.; Shah, S. *Orbital: Electron. J. Chem.* **2023**, *15*, 49. DOI: http://dx.doi.org/10.17807/orbital.v15i1.17592